

Article

Thermochemical Properties of PM_{2.5} as Indicator of Combustion Phase of Fires

Yuch-Ping Hsieh ^{1,*}, Glynnis Bugna ¹ and Kevin Robertson ²¹ Center for Water Resources, Florida A&M University, Tallahassee, FL 32307, USA; glynnis.bugna@famou.edu² Tall Timbers Research Station, Tallahassee, FL 32312, USA; krobertson@talltimbers.org

* Correspondence: yhsieh@famou.edu; Tel.: +1-850-599-3065

Received: 17 April 2018; Accepted: 28 May 2018; Published: 14 June 2018



Abstract: Past studies suggest that certain properties of fire emitted particulate matter (PM) relate to the combustion phase (flaming, smoldering) of biomass burning, but to date there has been little consideration of such properties for use as combustion phase indicators. We studied the thermochemical properties of PM_{2.5} emitted from experimental and prescribed fires using multi-element scanning thermal analysis (MESTA). Resulting thermograms show that the carbon from PM_{2.5} generally can be grouped into three temperature categories: low (peak ~180 °C), medium (peak between 180–420 °C), and high (peak > 420 °C) temperature carbons. PM_{2.5} from smoldering phase combustion is composed of much more low-temperature carbon (fraction of total carbon = 0.342 ± 0.067 , $n = 9$) than PM_{2.5} from the flaming phase (fraction of total carbon = 0.065 ± 0.018 , $n = 9$). The fraction of low-temperature carbon of the PM_{2.5} correlates well with modified combustion efficiency (MCE; $r^2 = 0.76$). Therefore, this MESTA thermogram method can potentially be used as a combustion phase indicator solely based on the property of PM_{2.5}. Since the MESTA thermogram of PM_{2.5} can be determined independently of MCE, we have a second parameter to describe the combustion condition of a fire, which may refine our understanding of fire behavior and improve the accuracy of emission factor determinations. This PM_{2.5} indicator should be useful for discerning differential diffusion between PM_{2.5} and gases and providing insight into the impact of PM emission on atmospheric environment and the public health.

Keywords: thermochemical property; particulate matter; combustion phase indicator; MESTA; emission factor; differential diffusion

1. Introduction

Estimating gaseous and particulate emissions to the atmosphere from wildland fire (wildfires and prescribed burns) remains a significant global challenge and high priority for air quality regulators, fire managers, and atmospheric scientists. Many such emissions are strongly influenced by phase of combustion of biomass during fires, specifically pyrolysis, flaming, smoldering, and glowing combustion, although the combustion phase is typically more broadly categorized as flaming or smoldering [1]. Flaming combustion is characterized by nearly complete combustion of volatilized fuel compounds through rapid oxidation producing visible flame and heat that sustains continued pyrolysis [2,3]. Smoldering combustion, which dominates after flaming combustion has ceased, involves a combination of pyrolysis without flame and char oxidation through glowing combustion in a relatively oxygen-limited environment and is characterized by lower rates of heat release and less complete combustion of volatilized gases and solids [4,5].

Although flaming and smoldering combustion phases are often separately described, in reality, especially in the case of wildland fire, these processes occur simultaneously, and their products are intermixed [2]. It is therefore important to estimate the relative contribution of each phase in

plumes of fire emissions. Smoldering combustion itself is a complex mixture of pyrolysis, glowing combustion of char, and occasional small flames, often occurring simultaneously in complex fuel beds made of particles with varying moisture content [1,5]. The most common continuous variable surrogate for degree of flaming versus smoldering combustion is combustion efficiency (CE), which is the ratio of carbon (C) released as carbon dioxide (CO₂) to C released in other chemical forms [2]. Modified combustion efficiency (MCE), which is the ratio of CO₂ emitted to the combined emissions of CO₂ and CO, is often used as a surrogate for CE, as CO₂ and CO are typically the dominant gas-phase products [6]. Strongly flaming-dominated combustion typically has values of MCE > 0.95 [7], while smoldering combustion with no visible flame usually has values of MCE < 0.90 [8], although this threshold varies among fuel types and fire conditions. Estimates of fire-emitted CO₂ and CO are generally made using the mass balance method [9], in which ambient concentrations of each gas are subtracted from concentrations measured in the emissions plume.

It is known that combustion phase influences the chemical composition of emissions [10]. Several gas-phase emission products have been shown to be positively correlated with MCE and thus are associated with flaming combustion, including nitric oxide (NO), nitrite (NO₂), hydrochloric acid (HCl), sulfur dioxide (SO₂), and nitrous acid (HONO) [5,11–14]. Other gas-phase emissions are negatively correlated with MCE and thus associated with smoldering combustion, including total non-methane hydrocarbons, ammonium (NH₃), methane (CH₄), ethane (C₂H₆), propene (C₃H₆), furan (C₄H₄O), acetic acid (CH₃COOH), formic acid (CH₂O₂), methanol (CH₃OH), bromomethane (CH₃Br), and formaldehyde (CH₂O) [5,8,12–18]. There is also evidence that combustion phase influences the chemical content of particulate matter (PM) emitted from biomass burning. Constituents of PM_{2.5} (particulate matter with aerodynamic diameter < 2.5 μm) positively associated with MCE and flaming combustion include elemental carbon (EC), ammonium, nitric oxide (NO), nitrite (NO₂), nitrate (NO₃⁻), sulfate (SO₄²⁻), oxalate (C₂O₄²⁻), K⁺, Cl⁻, S, and total inorganic aerosol species [10,17,19–21]. In contrast, PM_{2.5} produced by smoldering combustion is composed of relatively high percentages of organic carbon (OC), acetate ion (CH₃COO⁻), oxalate ion (C₂O₄²⁻), Ca, and Fe [10,12,17,19].

Given these trends, there is the possibility that the chemical composition of PM could be sufficiently related to the combustion phase to be used for estimating the relative contributions of flaming and smoldering combustion to the production of the PM. In past studies, emission factors for the EC and OC components of PM_{2.5} have been reported separately for combustion dominated by the flaming or smoldering phases, with fairly wide agreement that carbon from flaming combustion PM_{2.5} is ≥10% EC, and conversely carbon from smoldering combustion PM_{2.5} is >90% OC, often with little or no measurable EC [7,22]. Only one study to our knowledge reports the continuous relationship between EC fraction and MCE using multiple measurements [17], including single measurements made in other studies [23–27]. This study was consistent with others in that the 10% threshold of EC was at MCE of approximately 0.93, which is within the range of levels of MCE reported as the threshold between flaming- and smoldering-dominated combustion [7,25]. Given that there are practically no cases of pure flaming or smoldering combustion in wildland fires [2,22], MCE is important for expressing the relative strengths of these sources instead of simply classifying them as one or the other. The use of PM composition as a combustion phase indicator, once validated, could significantly improve estimates of emissions by employing appropriate EFs according to the weight of the dominant combustion phase without having to assume a lack of differential diffusion between PM and gas in the convection column [28]. However, given the considerable capacity for PM to accumulate OC during cooling and dispersion or to lose it through evaporation [22,29–31], relating thermochemical characteristics of PM to MCE requires special consideration of time since emission and specific atmospheric conditions during measurement, considered further in the discussion section.

Evolved gas analysis (EGA) has been used in the past as a method for fingerprinting aerosols from various sources according to the thermal stability of their compounds as measured by the evolution of the most common elements along a temperature ramp in the presence of an oxygen-containing

carrier [32–35]. In most studies of PM composition during the past decade, EGA methods have been used primarily as part of thermal-optical analysis (TOA) with the more specific goal of measuring amounts of EC and OC in PM samples. TOA methods involve measuring evolved C during a temperature ramp in the absence of oxygen to estimate OC, then measuring C in the presence of oxygen to measure EC using optical methods to correct for charring of OC during the first ramp [22,36].

Here, we present the multi-element scanning thermal analysis (MESTA) [35], for use in fingerprinting the thermochemical property of PM_{2.5} with regard to the combustion phase. Originally, MESTA was developed for analyzing complex mixtures of a solid sample [37]. MESTA heats a sample continuously at a constant rate with a carrier gas of fixed He/O₂ mixture. The approach of MESTA allows the compounds in a sample to be characterized and identified by the co-evolved C, N, and S thermograms when compared with those of known references running under the same heating rate and the same carrier gas. MESTA has been applied to the identification of black carbon [38]. However, in this study, the purpose is not to identify EC specifically but rather to produce a reliable thermal signature for combustion phase indication.

The purpose of this study is to empirically test the feasibility of MESTA thermograms of PM_{2.5} as an indicator of the combustion phase source of PM samples collected from a range of flaming to smoldering combustion conditions. Measurements involved both prescribed burning of natural fuels in southeastern US pine-grasslands and an outdoor controlled experiment using wood burning.

2. Experiments

2.1. Field Experiments

Field sampling of PM_{2.5} and combustion gases CO₂ and CO was conducted during prescribed burns in selected burn blocks located at Tall Timbers Research Station (TTRS), Tallahassee, FL, and Pebble Hill Plantation (PHP), Thomasville, GA. Study sites at TTRS and PHP included a wide range of upland forest land cover types representative of large areas of the southeastern U.S. Coastal Plain, including old-field (loblolly and shortleaf pine) and native (longleaf pine-wiregrass) upland pine-grasslands managed with frequent (1–2 year interval) prescribed fire and timber thinning (3–15 m²·ha⁻¹ tree basal area). Detailed characterization of prescribed burns conducted for this study along with other methods used are provided in previous studies [39].

For this study, we aimed to collect ground-based samples for PM_{2.5}, CO₂, and CO measurements during either predominantly flaming or predominantly smoldering combustion and for head fire and backing fire ignition techniques [40]. Flaming combustion samples were taken near the tip of the flames within the convection column, while smoldering combustion samples were taken within 50 cm of smoldering fuels within the plume of smoke after the flaming front had passed. Samples were collected through a hand-held galvanized aluminum tube from which a 30 m long flexible aluminum foil conduit (10 cm diameter) led to a sampling station outside of the burn unit [28]. A vent fan in series with the conduit was used to draw the air from the fire plume at 2200 L min⁻¹ into the top of a 50-cm diameter cylindrical sampling canopy (average 6.4 s transit time through conduit) that was open on the bottom to allow the free flow of air and PM into the surrounding air. Within the canopy were sampling ports for a PM_{2.5} sampler and a gas sampler. The PM_{2.5} sampler was a 16.7 L min⁻¹ EPA FEM air sampler configured with a very sharp cut cyclone (VSCC) device particle size separator (EQPM-0202-142, Mesa Laboratories, Inc., Butler, NJ, USA) with a thermometer recording the temperature of intake air. PM_{2.5} was collected on a pre-baked and pre-weighed quartz filter. The gas samples were collected at the rate of 450 mL min⁻¹ into a 10-L Tedlar air bag (Environmental Sampling Supply, Inc., San Leandro, CA, USA) for 3–5 min. Replicate (typically 3) PM_{2.5} and CO₂/CO samples were collected for each combustion phase. Prior to each burn, an ambient air sample was also collected in a 10-L Tedlar air bag for ambient CO₂ and CO measurements. We assume that there was little or no separation of the original emitted PM and gases from a fire when we sample them, which might occur through

differential diffusion of the products [28], as using a closed conduit from source to sampling location should maximize mixing and minimize separation of PM and gases in transit.

In the laboratory, the collected PM_{2.5} filter was equilibrated in a desiccator before weighing. PM samples were stored in the freezer prior to the multi-element scanning thermal analysis (MESTA). The CO₂ and CO samples were measured immediately using a LI-840A CO₂ analyzer (LI-COR, Inc., Lincoln, NE, USA) with a pump installed at the outlet and a Z-500XP CO meter with a built-in pump (Environmental Sensors Co.; Boca Raton, FL, USA), respectively. We used a certified mixture of CO₂/CO in nitrogen (Airgas, Inc., Tallahassee, FL, USA) for calibration of both instruments. During analyses we used lower concentrations of the certified 11% CO₂ standard (diluted with ultrapure CO₂-free air). We used the certified 50 ppm CO standard in a one-point calibration for analysis. The analytical accuracy of the CO₂ and CO analyzers are within ±0.3% and ±2%, respectively.

Modified Combustion Efficiency (MCE) values were calculated using the equation $MCE = \Delta CO_2 / (\Delta CO_2 + \Delta CO)$, where ΔCO_2 and ΔCO were differences in concentrations of fire emitted species between ambient and plume samples as conventionally measured [6].

2.2. Controlled Experiments

In addition to the field experiments, we also conducted a small scale wood burning experiment in an outdoor open-roof racquetball court. The goals were to determine: (1) the MESTA thermograms of a relatively pure flaming fire (MCE > 0.98) and a smoldering fire (MCE < 0.8), respectively; and (2) what happens to the smoldering PM, in term of the MESTA signature, after it is entrained into a convection column during flaming combustion. We set up two 120 L galvanized steel open-topped drums (trash cans each with four cut-out 10-cm square holes at the bottom), one for burning oak wood with flaming combustion (“flaming drum”) inside the racquetball court and another for burning wood with smoldering combustion (“smoldering drum”) 20 m outside of the court. Smoldering combustion was maintained by spraying flames with water. Outside of the court two PM and gas sampling stations (configured the same as in the field experiments described above) were set up about 35 m apart, one for sampling from the flaming drum and one for sampling from the smoldering drum, using flexible aluminum conduit (20–30 m length) and an in-series fan to direct air from each drum to its respective sampler. At the start of the experiment, we collected PM and gas samples from the both the flaming drum and the smoldering drum. We then directed smoke from the smoldering drum through a flexible aluminum conduit with an in-series fan to a hole in the base of the flaming drum to introduce the smoldering PM into the flaming drum. After three minutes, we re-directed the smoke from the smoldering drum directly to smoldering sampling station for another 3 min. This pair of measurements was repeated two more times but with different sampling periods (1.5 min and 1 min, respectively). For all experiments, PM_{2.5} and gas samples were collected, stored, and analyzed the same as for the field measurements.

2.3. Multi-Element Scanning Thermal Analysis (MESTA) of PM

MESTA was applied to the PM_{2.5} samples collected during the controlled and prescribed burn experiments. PM_{2.5} samples were removed from cold storage and placed in a desiccator in preparation for analysis. Each sample filter was cut into 16 pie-shaped pieces, two pieces were randomly selected and weighed. The weighed sample filters were then cut into much smaller pieces, placed in a quartz boat and into the MESTA device and analyzed in the temperature range from 35 °C to 700 °C under an ultrapure helium/oxygen (67%/33%) carrier gas. The volatilized sample was then carried into a 1070 °C main furnace fed with pure oxygen, in which the carbon, nitrogen and sulfur were oxidized into CO₂, NO₂, and SO₂, respectively. The oxidized gases then pass successively through detectors of CO₂ (infrared, IR analyzer, LI-COR, Inc., Lincoln, NE, USA), NO₂ (chemiluminescent detector, Petroleum Analyzer Co., Houston, TX, USA), and SO₂ (chemiluminescent detector, Petroleum Analyzer Co., Houston, TX, USA). The signals of the gases and the sample temperature were simultaneously recorded in a digital data logger, providing the result of the analysis. Standard

calibration curves of C and N of MESTA were obtained by mixtures of pure cystine and glucose standards. S was not detectable in the fire PM samples and, therefore, required no calibration. Total C and N concentrations of PM_{2.5} were calculated based on the fraction of the total filter and total PM_{2.5} weights used in the analysis among.

3. Results

3.1. MESTA Thermograms of PM_{2.5}

Figure 1A,B show examples of the C and N thermograms of PM_{2.5} collected from flaming phase and smoldering phases, respectively, from the outdoor controlled experiments. As found in previous experiments, the S content was negligible in samples collected from fire convection columns [35] and so is not reported. Figure 1C shows the C and N thermograms of the PM_{2.5} collected in the flaming fire plume with smoldering PM introduced at the base of the flame (smoldering/flaming).

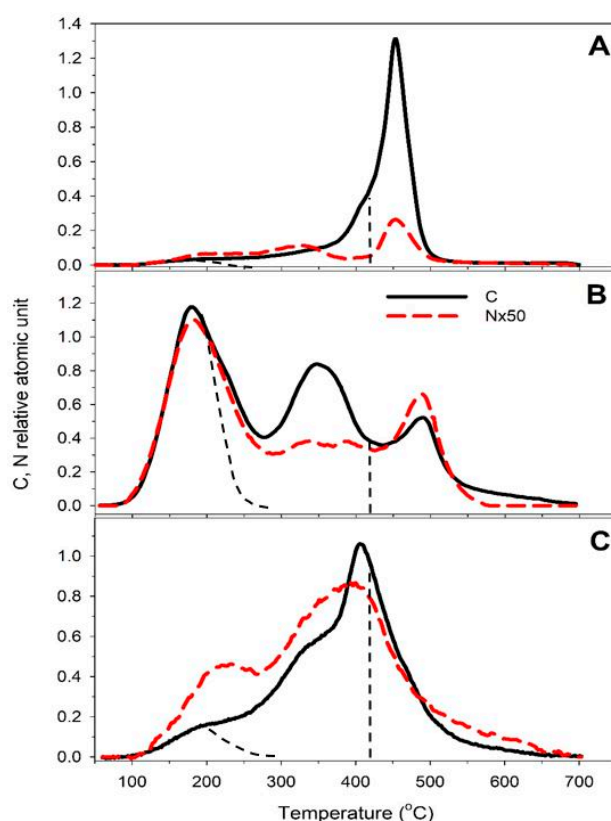


Figure 1. The typical C and N thermograms of flaming PM_{2.5} ((A) MCE = 0.98–0.99), smoldering PM_{2.5} ((B) MCE = 0.83–0.84), and the PM_{2.5} produced from the flaming drum after smoldering PM was introduced through the base of the drum ((C) MCE = 0.93–0.94). The C and N are plotted to their relative atomic unit scales; N is presented $\times 50$. Dashed black lines indicate the partitioning of the C fraction into low, medium, and high temperature categories as described in the text.

From the C thermograms, we can generally group the carbon into three categories according to the thermal stability (Figure 1, Table 1). We found that the low-temperature carbon peaks were relatively symmetrical and on average located at 180 ± 12.2 °C. Therefore, we quantify the low-temperature carbon fraction by identifying the low temperature peaks. If they were ≤ 180 °C, we integrated the area under the curve below the peak temperature and multiplied the value by two as the low-temperature carbon. If there was no obvious peak below 180 °C or peak above 180 °C, we then integrated the curve area below 180 °C and multiplied the value by two as the low-temperature

carbon. The high-temperature peaks were more diverse and non-symmetrical in comparison to the low-temperature peaks. Therefore, we simply integrated the area above 420 °C and defined it as the high-temperature carbon. The mid-temperature carbon was calculated as the difference between the total carbon and the sum of the low-temperature and the high-temperature carbons. The three carbons were expressed as the fractions of the total carbon.

Table 1. Summary of MCE and MESTA thermograph fractions of C volatilized at low, medium, and high temperatures (°C) for the controlled outdoor experiment using oak wood (Contr.) and field measurements in longleaf pine-grasslands (Field), mean with standard error of mean in parentheses.

Exp (<i>n</i>)	Phase	MCE	L (<180)	M (180–420)	H (>420)
Contr. (3)	Flaming	0.983 (0.004)	0.034 (0.007)	0.311 (0.134)	0.654 (0.143)
Contr. (3)	Smoldering	0.873 (0.034)	0.254 (0.052)	0.562 (0.048)	0.184 (0.008)
Contr. (3)	Mixed	0.969 (0.003)	0.054 (0.010)	0.547 (0.115)	0.399 (0.124)
Field (6)	Flaming	0.965 (0.003)	0.081 (0.024)	0.594 (0.053)	0.325 (0.051)
Field (6)	Smoldering	0.742 (0.042)	0.386 (0.074)	0.463 (0.059)	0.151 (0.021)
Field (17)	Mixed	0.932 (0.004)	0.088 (0.024)	0.604 (0.016)	0.307 (0.021)

The PM_{2.5} of the flaming, smoldering and the smoldering/flaming samples can be distinguished by their characteristic C thermograms: The PM_{2.5} of flaming phase samples (MCE = 0.97 ± 0.01) was dominated by the high-temperature carbon. The PM_{2.5} of smoldering phase samples (MCE = 0.74 ± 0.10) was dominated by the low-temperature carbon, although high and mid-temperature carbons were still evident. The interpretation of the thermogram in Figure 1C is more complicated because it was from the smoldering PM entrained in the flaming drum in which the flaming PM also contributed. PM_{2.5} from the smoldering drum had an EF of 131 ± 43.2 mg kg⁻¹ (MCE = 0.84 ± 0.01), whereas PM_{2.5} from the flaming drum had an EF of 2.5 ± 0.6 mg kg⁻¹ (MCE = 0.98 ± 0.01). After introducing the smoldering PM to the flaming drum, the PM_{2.5} EF increased from 2.5 ± 0.6 mg kg⁻¹ to 50.6 ± 3.8 mg kg⁻¹ (MCE = 0.92 ± 0.02). These results suggest that the source of PM_{2.5} in Figure 1C must be mainly from the smoldering PM that passed through the flaming drum, because the residual smoldering PM_{2.5} overwhelmed the flaming PM_{2.5} by 20 times. By our estimation, the mean residence time of the smoldering PM in the flaming drum was very short, within a few seconds. However, the change in the MESTA thermogram was pronounced, in that most of the low-temperature carbon, as well as the smaller fraction of high-temperature carbon, had mostly disappeared (Compare Figure 1B to Figure 1C).

Differences between the flaming and smoldering thermograms can be seen in the fraction of low-temperature carbon alone, where their fraction for the smoldering phase was 0.342 ± 0.067 (*n* = 9) whereas that for the flaming phase was 0.065 ± 0.018 (*n* = 9). Another difference between the thermograms is the higher nitrogen content of the smoldering PM_{2.5} compared to the flaming PM_{2.5}. The average C/N ratio of the PM_{2.5} from the smoldering phase was 55.7 ± 5.2, whereas that of the flaming phase was 131.2 ± 20.0. When the smoldering PM was fed into the flaming fire, both the low-temperature and high-temperature carbon of the smoldering PM_{2.5} were relatively muted, leaving the medium-temperature carbon to dominate (Figure 1C). The nitrogen content of smoldering/flaming PM_{2.5} was also greater than in either the smoldering or flaming PM (C/N ratio = 41.4 ± 2.1 compared to 55.7 ± 5.2 and 131.2 ± 20.0). We are not sure why carbon and nitrogen were differentially consumed when the smoldering PM passed through the flaming drum.

Figure 2 shows some examples of PM_{2.5} thermograms from the field experiments. The top two (A and B) were sampled from flaming-dominated fire, the middle two (C and D) were from the smoldering combustion only, and the bottom two (E and F) were from flaming fires with intermediate levels of MCE (0.90–0.95), suggesting that these samples (E and F) were mixed with considerable smoldering, similar to the smoldering/flaming treatment in the controlled experiment.

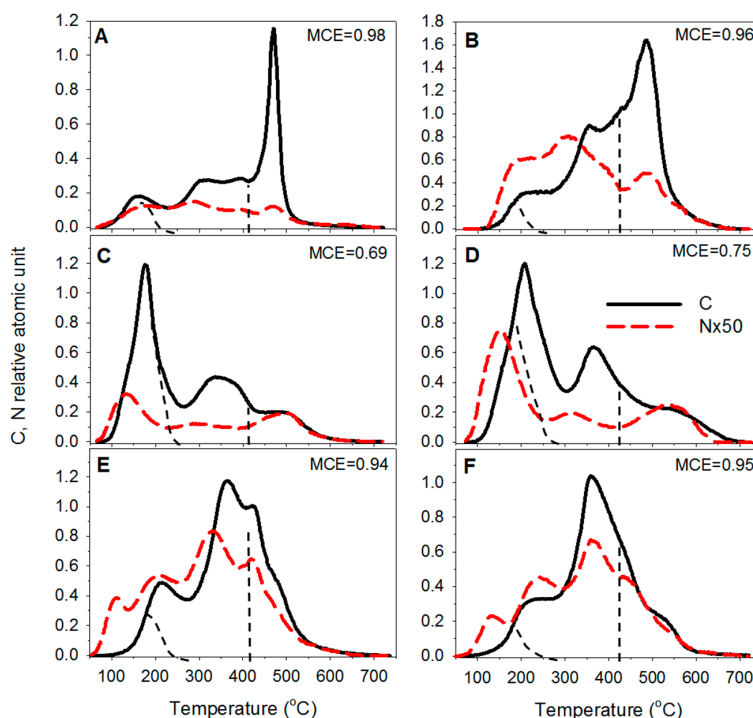


Figure 2. Some examples of C and N thermograms of the field experiments, including flaming dominated combustion (A,B), smoldering dominated combustion (C,D), and mixed combustion phase (E,F). The C and N are plotted to their relative atomic unit scales; N is presented $\times 50$. Dashed black lines indicate the partitioning of the C fraction into low, medium, and high temperature categories as described in the text.

3.2. The MESTA Thermogram of $PM_{2.5}$ and MCE of Gases

Figure 3 shows the relationship between the fraction of the low-temperature carbon of $PM_{2.5}$ and the corresponding MCE of the gases collected simultaneously during the experiments. The linear regression was significant with r -square of 0.76. The regression slope is negative because a higher fraction of the low-temperature carbon indicates lower MCE.

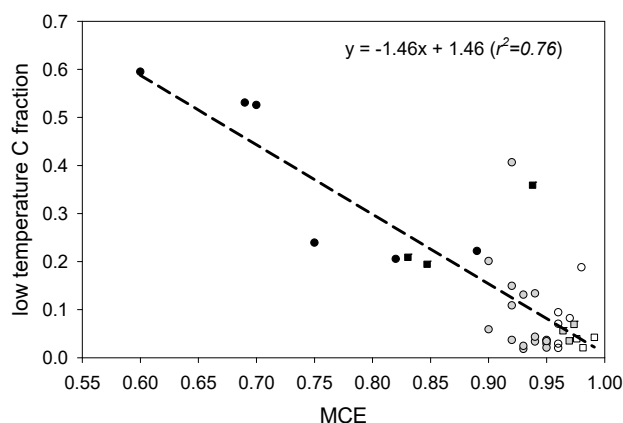


Figure 3. Relationship between MCE of gases and the fraction of low-temperature carbon determined by MESTA. Round symbols = field measurements; square symbols = outdoor controlled experiment. Open circle = flaming combustion; gray fill = flaming with added smoldering PM in controlled experiments or flaming with intermediate MCE (0.90–0.95) in field measurements; black fill = smoldering combustion.

Figure 4 shows the relationship between the fraction of low-temperature carbon and that of the high-temperature carbon in the PM_{2.5} collected from the field experiments. According to MCE levels measured in the field, the smoldering combustion phase (MCE < 0.90) is represented by symbols in the lower region, the flaming combustion phase (MCE > 0.95) is represented by symbols in the upper left corner, and mixed samples are represented by symbols in between.

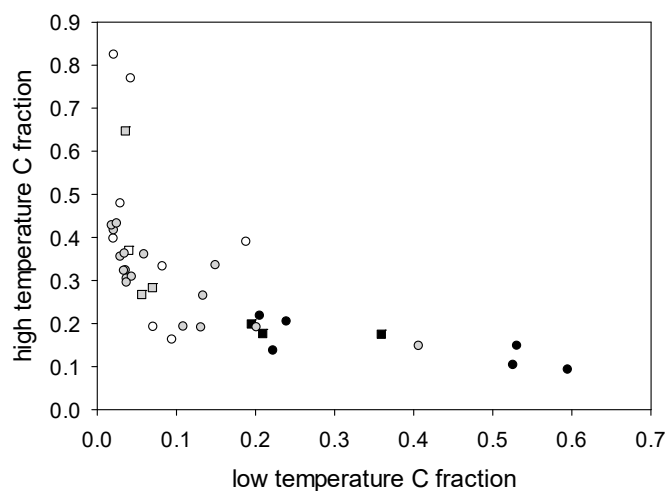


Figure 4. The relationship between the fractions of low-temperature carbon (peak at 180 °C) and the high-temperature carbon (>420 °C) of the PM_{2.5} collected in the field experiments. Round symbols = field measurements; square symbols = outdoor controlled experiment. Open circle = flaming combustion; gray fill = flaming with added smoldering PM in controlled experiments or flaming with intermediate MCE (0.90–0.95) in field measurements; black fill = smoldering combustion.

4. Discussion

The results of our study suggest that C and N thermograms of PM_{2.5} derived from MESTA might be used to differentiate the combustion phase by which PM was emitted, at least for the fuel types used here, although the results are preliminary to field application. The thermograms provide more information than what might be revealed by MCE alone. The thermograms are basically super positioned in nature (data not shown). For example, we could have a mixture of Figure 1A and B that has a MCE of 0.93–0.94 and with a thermogram showing both significant low-temperature and high-temperature carbon peaks, if the smoldering and flaming PM had mixed in the cooled plume. On the other hand, we had the PM with the same MCE (0.93–0.94) but with both insignificant low-temperature and high-temperature carbons as shown in Figure 1C because the smoldering PM had gone through a flaming fire.

Another advantage of MESTA is that it provides the co-evolved nitrogen and possibly hydrogen, which would be valuable in understanding the nature of PM and its relevance to air quality, although this is outside the scope in this report.

MCE and MESTA thermogram are both combustion phase indicators, one for gases and one for PM, that each can be determined independently. MCE is a single-value indicator whereas MESTA thermograms have multiple constraints in describing a combustion condition of a fire. Using both indicators to describe the combustion phase of fire may refine our understanding of the combustion phase of a fire and may even improve the accuracy of PM emission factor (EF) estimation.

A general challenge facing the application of these methods as a valid combustion phase indicator is the possible changes in the chemical nature of PM among different sampling locations and time since emission from the fire could change the MESTA thermogram of PM. Other studies have reported that PM could change in composition through condensation of volatile organic compounds on initially

emitted particles, as well as the potential for subsequent evaporation of such compounds [22,29,30]. PM typically develops from condensation of relatively volatile organic compounds on thermally stable carbon compounds that serve as condensation nuclei, such that the low thermal stability component increases as particles accumulate. The rate and degree of accumulation depends on a combination of temperature and PM concentration, where accumulation is promoted by falling temperature but countered by decreasing concentration as PM disperses in the atmosphere [31]. The most rapid changes are immediately following emission from the flaming zone as gases and PM rapidly cool and disperse in the convection column. Subsequent changes, including evaporation of volatile organics and adsorption of inorganic nitrogen and sulfur compounds to form secondary aerosols, occur much more slowly, typically over days rather than seconds or minutes [22].

Although the effect of changes in the chemical property of PM_{2.5} within the convection column on the stability of the MESTA thermograms will require further empirical investigation, several aspects of presented method likely mitigate the most important challenges. The PM sampler thermometer recorded gas temperatures at the intake to be an average of 30.4 ± 4.2 °C for flaming combustion samples and 30.1 ± 4.2 °C for smoldering combustion samples, within 1 °C of ambient air temperature. Measurements using high-temperature thermocouples during the field experiments [39] showed the maximum air temperature within the flaming zone to typically be in the range of 800–1200 °C. The rapid cooling during the average 6.4 s of transit time from the flame to the sample in field samples may be explained by the rapid expansion of the gas (a refrigeration effect) from the outlet of the conduit to the collection canopy, which may mimic cooling in the convection column to a more stable PM composition. Given that concentrations of PM_{2.5} at the sampling station were an average of 56 ± 33 mg m⁻³ for flaming combustion samples and 273 ± 272 mg m⁻³ for smoldering combustion, equations relating temperature and PM_{2.5} concentration to the fraction of semi-volatile organic compounds in the particle phase [30] predict >85% of such compounds in this study to be in the particle phase. Also, the quartz filters used to collect PM may have also collected artifacts of semi-volatile organic compounds in the gas phase at the time of collection [36]. Whereas such artifacts are a problem for quantifying particle phase emissions, in this case they may provide a more inclusive sample of potentially absorbed carbon compounds for the purposes of analysis of thermochemical property. Finally, although particle size has been recorded to grow to as much as double their initial size within 2 h of emission within the convection column of wildland fires [3,40,41], much of the accumulation can be attributed to water absorption and coagulation of existing particles, which would not influence measurement of the MESTA carbon thermogram. For example, measurements taken during a prescribed burn showed that 84% of particle growth was because of water absorption facilitated by high relative humidity in the convection column [3]. Our samples are desiccated prior to analysis using MESTA so that water content has no influence on the elements measured. We did examine the consistency of the PM thermograms after periods of storage and found them very consistent even after three years. Nevertheless, methods presented here for using the MESTA thermogram of PM_{2.5} as a combustion phase indicator should be confirmed through further experiments that check its consistency by simultaneously sampling PM at various positions and time.

The analysis of PM collected on filters may have some advantages over real-time measurements designed to quantify PM composition. Most such analyzers depend on a combination of light scattering, which responds to particle size, and light absorption, assumed to be determined primarily by the fraction of EC [10]. As discussed above, particle size is generally a more fluid characteristic of PM than thermal stability of constituent carbon compounds [3]. Also, information contained in variation in thermal stability among OC constituents indicated by thermograms might be missed by measurements of light absorption, assuming the latter is mostly dependent on the EC fraction [10].

Research to date has typically categorized carbon compounds in PM samples as organic and elemental carbons. The so called “elemental” carbon is the pyrolysis product of organic carbon, in which pyrolysis eliminates most of other elements such as oxygen, nitrogen, and hydrogen from the carbon compounds, leaving mainly carbons representing various degrees of condensation [38].

The “elemental” carbon, therefore, is a loosely defined term representing a spectrum of relatively pure carbon compounds in various degrees of condensation [38,42]. Although elemental carbon has been conceptually and agreeably defined, it has not been analytically and agreeably defined [38,42]. Generally, more condensed forms of carbon would show more thermal stability [38,42]. Judging from these criteria, the thermograms show that the smoldering PM_{2.5} probably contains little elemental carbon. Although some carbon is thermally stable above 450 °C (Figure 1B,C), the co-evolved nitrogen showed a C/N ratio of 44.8 ± 7.8 , suggesting that the carbon is not likely to be classified as elemental. On the other hand, the PM_{2.5} emitted from flaming combustion phase contains some elemental carbon, judging from its thermal stability and high C/N ratios (258.8 ± 99.6) in the high temperature category.

In Figure 3, there are three measurements in particular that are outliers in the direction of higher low temperature C fraction relative to MCE as compared to the other measurements, specifically 0.41, 0.36, and 0.19 at values of MCE of 0.92, 0.94, and 0.98, respectively. These include two that are field measurements of flaming-dominated combustion and one that was a measurement of smoldering combustion in the controlled experiment. We speculate that, despite our effort to minimize the differential diffusion between PM and CO₂ in our experiments, there still may have few “mis-matched” samples. It is also possible that there are variations in the chemical composition of the fuels that might translate into composition of PM in a manner that is not reflected by MCE, although this seems unlikely in the case of the controlled experiments, given that all of the fuel (oak wood) was from the same source.

Figure 5 shows three thermograms that differ in their signature but the same MCE (0.95). MCE is a single-value indicator of gases and thus has limited ability to describe a mixed combustion phase. The MESTA thermogram, on the other hand, has multiple constraints providing more information about the mixing of combustion phases. In this report, we use only three simple categories of carbons to show its potential as a multi-constraint indicator. It may have more useful carbons and nitrogen constraints that can be used to indicate the combustion condition of a fire, although further study is needed to understand how they can be used and interpreted. However, the low temperature C component found in this study is likely to provide the best indication that matches MCE among these measurements.

The relationship between the low-temperature C of PM_{2.5} and MCE identified in this study might differ among fuel types. PM has been shown to vary widely in its relative amounts of OC and EC [17,23], reflecting fundamental differences in fuel chemistry and/or combustion processes, although variation in thermal stability among constituents composing OC are generally not reported. Apart from the three outliers in our study mentioned above, the relationship between the low temperature C of PM_{2.5} and MCE (Figure 3) appeared to be similar between the wood burned in the controlled experiments and the fuels in the field composed mostly of grass, forbs, and pine needles [39]). This pattern suggests the robustness of this approach to different fuel types, but these results are limited in scope and beg further empirical studies.

Our controlled experiment demonstrated the potential for products of smoldering combustion to be entrained in the flaming combustion column and thereby influence the salient thermochemical characteristics of the PM. This observation demonstrates the potential complexity of emissions from wildland fires and helps to explain the wide range of PM_{2.5} EFs measured among fires dominated by flaming combustion [17,21]. Fire behavior, convective fluid dynamics of the fire environment, and potential for smoldering of fuels immediately after passage of the flaming front may influence the chemical composition and quantity of emissions entrained and transported convectively by flame-driven plumes.

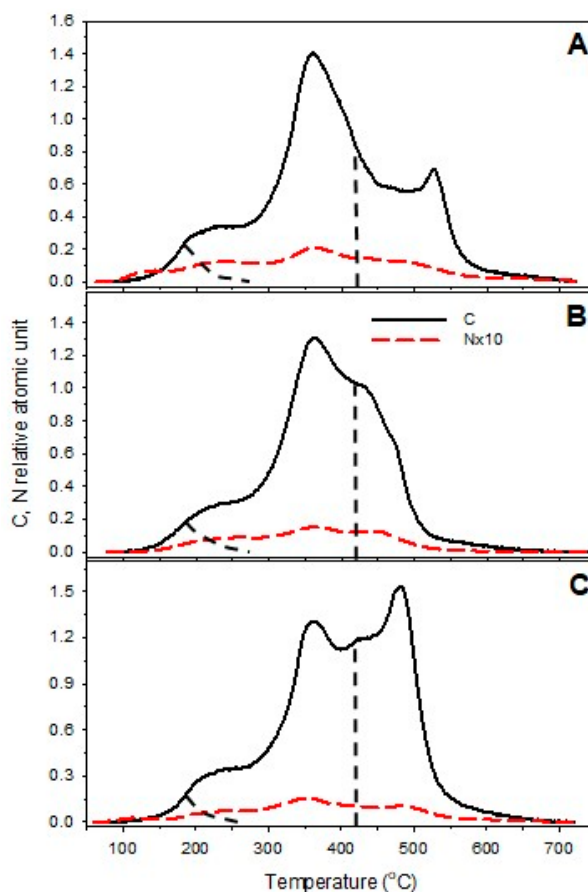


Figure 5. Examples of the various C and N thermograms of PM_{2.5} samples with MCE = 0.95. The C and N are plotted to their relative atomic unit scales; N is presented $\times 10$. Dashed black lines indicate the partitioning of the C fraction into low, medium, and high temperature categories as described in the text.

5. Conclusions

We have identified a PM_{2.5} combustion phase indicator, which is the MESTA carbon thermogram. The PM_{2.5} emitted from a flaming fire has a high proportion of high-temperature (>420 °C) volatile carbon in its carbon MESTA thermogram, whereas that emitted from a smoldering fire is dominated by low-temperature (peaks around 180 °C) volatile carbon. After PM from smoldering combustion passed through a flaming fire, its MESTA carbon thermogram changed, in that both the low-temperature and high-temperature carbon peaks were reduced, leaving a dominant medium-temperature carbon peak. This PM combustion phase indicator can be applied independent of MCE, which is the gas-phase combustion phase indicator. This application may be particularly useful where the assumption of thorough mixing of gas and PM is weak, as in the case of smoldering combustion with weak convection columns and low turbulence. For calibration purposes, using this indicator in conjunction with MCE can ensure a matched pair of PM and gas samples to confirm the assumption of thorough mixing, which is a key assumption for accurately determining emission factors. This check may be important given that mixing of PM and gas samples in a fire experiment is not guaranteed even for simultaneously collected samples due to the possible differential diffusion effect between the two [28].

Compared to typical measurements of PM chemical composition, the MESTA thermogram of PM_{2.5} provides a rich source of information that may be utilized to identify the dominant combustion phase of wildland fire and perhaps other characteristics of the PM emitted from a fire. The possible use of the co-evolved elements such as N and possibly H might also be helpful in characterizing

the sources and chemical composition of PM, a fire product with global significance to atmospheric processes and human health.

Author Contributions: Y.-P.H. and K.R. conceived and designed the experiments. Y.-P.H., G.B. and K.R. performed the experiments, analyzed the data and wrote the paper.

Acknowledgments: We would like to thank the research staff and students from Florida A&M University and Tall Timbers Research Station for their help in the field and laboratory. We would like to thank the National Science Foundation for funding this work. Support for this research was provided by NSF Award # 0962970 to Y.-P.H., K.R. and G.B. We would also like to thank the two anonymous reviewers whose suggestions and comments greatly improved this manuscript.

Conflicts of Interest: The authors declare no conflict of interest.

References

1. Urbanski, S.P. Wildland fire emissions, carbon, and climate: Emission factors. *For. Ecol. Manag.* **2014**, *317*, 51–60. [[CrossRef](#)]
2. Ward, D.E.; Hardy, C.C. Smoke emissions from wildland fires. *Environ. Int.* **1991**, *17*, 117–134. [[CrossRef](#)]
3. Hobbs, P.V.; Reid, J.S.; Herring, J.A.; Nance, J.D.; Weiss, R.E.; Ross, J.L.; Hegg, D.A.; Ottmar, R.D.; Lioussé, C. Particle and trace-gas measurements in the smoke from prescribed burns of forest products in the Pacific Northwest. In *Biomass Burning and Global Change*; MIT Press: Cambridge, MA, USA, 1996.
4. Ward, D.E.; Peterson, J.; Hao, W.M. An inventory of particulate matter and air toxic emissions from prescribed fires in the USA for 1989. In Proceedings of the Air and Waste Management 86th Annual Meeting, Denver, CO, USA, 13–18 June 1993.
5. Burling, I.R.; Yokelson, R.J.; Griffith, D.W.T.; Johnson, T.J.; Veres, P.; Roberts, J.M.; Warneke, C.; Urbanski, S.P.; Reardon, J.; Weise, D.R.; et al. Laboratory measurements of trace gas emissions from biomass burning of fuel types from the southeastern and southwestern United States. *Atmos. Chem. Phys.* **2010**, *10*, 11115–11130. [[CrossRef](#)]
6. Urbanski, S.P. Combustion efficiency and emission factors for wildfire-season fires in mixed conifer forests of the northern Rocky Mountains, US. *Atmos. Chem. Phys.* **2013**, *13*, 7241–7262. [[CrossRef](#)]
7. Battye, W.; Battye, R. *Development of Emissions Inventory Methods for Wildland Fire. Final Report. EPA Contract No. 68-D-98-046. Work Assignment No. 5-03*; EC/R Inc.: Durham, NC, USA, 2002.
8. Bertschi, I.T.; Yokelson, R.J.; Ward, D.E.; Babbitt, R.E.; Susott, R.A.; Goode, J.G.; Hao, W.M. Trace gas and particle emissions from fires in large diameter and belowground biomass fuels. *J. Geophys. Res.* **2003**, *108*. [[CrossRef](#)]
9. Radke, L. Particulate and trace gas emission from large biomass fires in North America. In *Global Biomass Burning: Atmospheric Climatic and Biospheric Implications*; MIT Press: Cambridge, MA, USA, 1991.
10. Reid, J.S.; Eck, T.F.; Christopher, S.A.; Koppmann, R.; Dubovik, O.; Eleuterio, D.P.; Holben, B.N.; Reid, E.A. A review of biomass burning emissions part III: Intensive optical properties of biomass burning particles. *Atmos. Chem. Phys.* **2005**, *5*, 827–849. [[CrossRef](#)]
11. Yokelson, R.J.; Griffith, D.W.T.; Ward, D.E. Open-path Fourier transform infrared studies of large-scale laboratory biomass fires. *J. Geophys. Res.* **1996**, *101*, 21067–21080. [[CrossRef](#)]
12. Ferek, R.J.; Reid, J.S.; Hobbs, P.V.; Blake, D.R.; Lioussé, C. Emission factors of hydrocarbons, halocarbons, trace gases and particles from biomass burning in Brazil. *J. Geophys. Res.* **1998**, *103*, 32107–32118. [[CrossRef](#)]
13. Alves, C.A.; Goncalves, C.; Pio, C.A.; Mirante, F.; Caseiro, A.; Tarelho, L.; Freitas, M.C.; Viegas, D.X. Smoke emissions from biomass burning in a Mediterranean shrubland. *Atmos. Environ.* **2010**, *44*, 3024–3033. [[CrossRef](#)]
14. Yokelson, R.J.; Burling, I.R.; Gilman, J.B.; Warneke, C.; Stockwell, C.E.; de Gouw, J.; Akagi, S.K.; Urbanski, S.P.; Veres, P.; Roberts, J.M.; et al. Coupling field and laboratory measurements to estimate the emission factors of identified and unidentified trace gases for prescribed fires. *Atmos. Chem. Phys.* **2013**, *13*, 89–116. [[CrossRef](#)]
15. Yokelson, R.J.; Bertschi, I.T.; Christian, T.J.; Hobbs, P.V.; Ward, D.E.; Hao, W.M. Trace gas measurements in nascent, aged, and cloud-processed smoke from African savanna fires by airborne Fourier transform infrared spectroscopy (AFTIR). *Geophys. Res.* **2003**, *108*. [[CrossRef](#)]

16. Yokelson, R.J.; Karl, T.; Artaxo, P.; Blake, D.R.; Christian, T.J.; Griffith, D.W.T.; Guenther, A.; Hao, W.M. The tropical forest and fire emissions experiment: Overview and airborne fire emission factor measurements. *Atmos. Chem. Phys.* **2007**, *7*, 5175–5196. [[CrossRef](#)]
17. McMeeking, G.R.; Kreidenweis, S.M.; Baker, S.; Carrico, C.M.; Chow, J.C.; Collett, J.L.J.; Wei, M.H.; Holden, A.S.; Kirchstetter, T.W.; Malm, W.C.; et al. Emissions of trace gases and aerosols during the open combustion of biomass in the laboratory. *J. Geophys. Res.* **2009**, *114*. [[CrossRef](#)]
18. Burling, I.R.; Yokelson, R.J.; Akagi, S.K.; Urbanski, S.P.; Wold, C.E.; Griffith, D.W.T.; Johnson, T.J.; Reardon, J.; Weise, D.R. Airborne and ground-based measurements of the trace gases and particles emitted by prescribed fires in the United States. *Atmos. Chem. Phys.* **2011**, *11*, 12197–12216. [[CrossRef](#)]
19. Yamasoe, M.A.; Artaxo, P.; Miguel, A.H.; Allen, A.G. Chemical composition of aerosol particles from direct emissions of vegetation fires in the Amazon Basin: Water-soluble species and trace elements. *Atmos. Environ.* **2000**, *34*, 1641–1653. [[CrossRef](#)]
20. Lee, T.; Sullivan, A.P.; Mack, L.; Jimenez, J.L.; Kreidenweis, S.M.; Onasch, T.B.; Worsnop, D.R.; Malm, W.C.; Wold, C.E.; Wei, M.H.; et al. Chemical smoke marker emissions during flaming and smoldering phases of laboratory open burning of wildland fuels. *Aerosol Sci. Technol.* **2010**, *44*. [[CrossRef](#)]
21. Aurell, J.; Gullett, B.K. Emission factors from aerial and ground measurements of field and laboratory forest burns in the southeastern U.S.: PM_{2.5}, black and brown carbon, VOC, and PCDD/PCDF. *Environ. Sci. Technol.* **2013**, *47*, 8443–8452. [[CrossRef](#)] [[PubMed](#)]
22. Reid, J.S.; Koppmann, R.; Eck, T.F.; Eleuterio, D.P. A review of biomass burning emissions part II: Intensive physical properties of biomass burning particles. *Atmos. Chem. Phys.* **2005**, *5*, 799–825. [[CrossRef](#)]
23. Chen, L.W.A.; Moosmuller, H.; Arnott, W.P.; Chow, J.C.; Watson, J.G.; Susott, R.A.; Babbitt, R.E.; Wold, C.E.; Lincoln, E.N.; Wei, M.H. Emissions from laboratory combustion of wildland fuels: Emission factors and source profiles. *Environ. Sci. Technol.* **2007**, *41*, 4317–4325. [[CrossRef](#)] [[PubMed](#)]
24. Andreae, M.O.; Merlet, P. Emission of trace gases and aerosols from biomass burning. *Glob. Biogeochem. Cycles* **2001**, *15*, 955–966. [[CrossRef](#)]
25. Hays, M.D.; Geron, C.D.; Linna, K.J.; Smith, D.; Schauer, J.J. Speciation of gas-phase and fine particle emissions from burning of foliar fuels. *Environ. Sci. Technol.* **2002**, *36*, 2281–2295. [[CrossRef](#)] [[PubMed](#)]
26. Christian, T.J.; Kleiss, B.; Yokelson, R.J.; Holzinger, R.; Crutzen, P.J.; Hao, W.M.; Saharjo, B.H.; Ward, D.E. Comprehensive laboratory measurements of biomass-burning emissions: 1. Emissions from Indonesian, African, and other fuels. *J. Geophys. Res. Atmos.* **2003**, *108*. [[CrossRef](#)]
27. Iinuma, Y.; Brüggermann, E.; Gnauk, T.; Müller, K.; Andreae, M.O.; Helas, G.; Parmar, R.; Hermann, H. Source characterization of biomass burning particles: The combustion of selected European conifers, African hardwood, savanna grass, and German and Indonesian peat. *J. Geophys. Res.* **2007**, *112*. [[CrossRef](#)]
28. Hsieh, Y.P.; Bugna, G.C.; Robertson, K.M. Examination of two assumptions commonly used to determine PM_{2.5} emission factors for wildland fires. *Atmos. Environ.* **2016**, *147*, 274–283. [[CrossRef](#)]
29. Robinson, A.L.; Brieshop, A.P.; Donahue, N.M.; Hunt, S.W. Updating the conceptual model for fine particle mass emissions from combustion systems. *J. Air Waste Manag. Assoc.* **2010**, *60*, 1204–1222. [[CrossRef](#)] [[PubMed](#)]
30. May, A.A.; Levin, E.J.T.; Hennigan, C.J.; Riipinen, I.; Lee, T.; Collett, J.L., Jr.; Jimenez, J.L.; Kreidenweis, S.M.; Robinson, A.L. Gas-particle partitioning of primary organic aerosol emissions: 3. Biomass burning. *J. Geophys. Res. Atmos.* **2013**, *118*, 11327–11338. [[CrossRef](#)]
31. Lipsky, E.M.; Robinson, A.L. Effects of dilution on fine particle mass and partitioning of semivolatile organics in diesel exhaust and woody smoke. *Environ. Sci. Technol.* **2006**, *40*, 155–162. [[CrossRef](#)] [[PubMed](#)]
32. Grosjean, D.; Williams, E.L.I.; Grosjean, E.; Novakov, T. Evolved gas analysis of secondary organic aerosols. *Aerosol Sci. Technol.* **1994**, *21*, 306–324. [[CrossRef](#)]
33. Ellis, E.C.; Novakov, T. Application of thermal analysis to the characterization of organic aerosol particles. *Sci. Total Environ.* **1982**, *23*, 227–238. [[CrossRef](#)]
34. Turner, J.R.; Hering, S.V. Vehicle contribution to ambient carbonaceous aerosols by scaled thermograms. *Aerosol Sci. Technol.* **2007**, *12*, 620–629. [[CrossRef](#)]
35. Hsieh, Y.P.; Bugna, G.C.; Robertson, K.M. Chemical signature of biomass burning-emitted PM_{2.5} and the detection of its presence in the air by a rapid method. *Tall Timbers Fire Ecol. Conf. Proc.* **2010**, *24*, 73–78.
36. Turpin, B.J.; Saxena, P.; Andrews, E. Measuring and simulating particulate organics in the atmosphere: Problems and prospects. *Atmos. Environ.* **2000**, *34*, 2983–3013. [[CrossRef](#)]

37. Hsieh, Y.P. A novel multielemental scanning thermal analysis (MESTA) method for the identification and characterization of solid substances. *J. AOAC Int.* **2007**, *90*, 54–59. [[PubMed](#)]
38. Hsieh, Y.P.; Bugna, G.C. Analysis of black carbon in sediments and soils using multi-element scanning thermal analysis (MESTA). *Org. Chem.* **2008**, *39*, 1562–1571. [[CrossRef](#)]
39. Robertson, K.M.; Hsieh, Y.P.; Bugna, G.C. Fire environment effects on particulate matter emission factors in southeastern U.S. pine-grasslands. *Atmos. Environ.* **2014**, *99*, 104–111. [[CrossRef](#)]
40. Kaufman, Y.J.; Hobbs, P.V.; Kirchhoff, V.W.J.H.; Artaxo, P.; Remer, L.A.; Holben, B.N.; King, M.D.; Ward, D.E.; Prins, E.M.; Longo, K.M.; et al. Smoke, clouds, and radiation—Brazil (SCAR-B) experiment. *J. Geophys. Res.* **1998**, *103*, 31783–31808. [[CrossRef](#)]
41. Fraser, M.P.; Kleeman, M.J.; Schauer, J.J.; Cass, G.R. Modeling the atmospheric concentrations of individual gas-phase and particle-phase organic compounds. *Environ. Sci. Technol.* **2000**, *34*, 1302–1312. [[CrossRef](#)]
42. Leiffield, J. Thermal stability of black carbon characterised by oxidative differential scanning calorimetry. *Org. Geochem.* **2007**, *38*, 112–127. [[CrossRef](#)]



© 2018 by the authors. Licensee MDPI, Basel, Switzerland. This article is an open access article distributed under the terms and conditions of the Creative Commons Attribution (CC BY) license (<http://creativecommons.org/licenses/by/4.0/>).